Including vegetation dynamics in an atmospheric chemistry-enabled GCM: Linking LPJ-GUESS (v4.0) with EMAC modelling system (v2.53)

Matthew Forrest[1,2], Holger Tost[3], Jos Lelieveld[2,4], and Thomas Hickler[1,5]

[1]Senckenberg Biodiversity and Climate Research Centre (SBiK-F), Frankfurt am Main, Germany
[2]Atmospheric Chemistry Department, Max Planck Institute for Chemistry, Mainz, Germany
[3]Institute for Atmospheric Physics, Johannes Gutenberg University Mainz, Mainz, Germany
[4]Energy, Environment and Water Research Center, The Cyprus Institute, Nicosia, Cyprus
[5]Institute for Physical Geography, Goethe University, Frankfurt am Main, Germany

Correspondence to: Matthew Forrest (matthew.forrest@senckenberg.de)

Abstract.

Central to the development of Earth System Models (ESMs) has been the coupling of previously separate model types, such as ocean, atmospheric and vegetation models, to provide interactive feedbacks between the system components. A modelling framework which combines a detailed representation of these components, including vegetation and other land surface processes, enables the study of land-atmosphere feedbacks under global change. This includes the methane cycle and lifetime and the atmospheric chemistry of reduced carbon; fire effects and feedbacks; future nitrogen deposition rates and fertilisation scenarios; ozone damage to plants; and the contribution of biogenic volatile organic compounds to aerosol load and, via cloud condensation nuclei activation, to cloud formation (e.g., precipitation cycles). Here we present the initial steps of coupling LPJ-GUESS, a dynamic global vegetation model, to the atmospheric chemistry enabled atmosphere-ocean general circulation model EMAC. The LPJ-GUESS framework includes a comparatively detailed individual based model of vegetation dynamics, a crop and managed-land scheme, a nitrogen cycle and a choice of fire models; and hence represents many important terrestrial biosphere processes and provides a wide range of prognostic trace gas emissions from vegetation, soil and fire. When development is complete, these trace gas emissions will form key inputs to the state-of-art atmospheric chemistry representations in EMAC allowing for bi-directional chemical interactions of the surface with the atmosphere. Then the full model will become a powerful tool for investigating land-atmosphere interactions. Initial results show that the one-way, on-line coupling from EMAC to LPJ-GUESS gives a reasonable description of the global potential natural vegetation distribution and reproduces the broad patterns of biomass, tree cover and canopy height when compared to remote sensing datasets. Based on this first evaluation, we conclude that the coupled model provides a suitable means to simulate dynamic vegetation processes into EMAC.

1 Introduction

Simulation models are at the forefront of earth systems research. Historically, such models were initially developed to simulate one component of the earth system in isolation, such as ocean and atmospheric General Circulation Models (GCMs) or Dynamic Global Vegetation Models (DGVMs), with prescribed boundary conditions at the interfaces to other earth system components. However, the interactions between earth system components are dynamic, and representations of feedbacks are necessary to assess the functioning and response of the earth system as a whole. To this end, simulations models have increasingly been coupled to each other to provide dynamic multidirectional fluxes between models, as opposed to prescribing simple non-interacting boundary conditions. This approach has yielded Atmosphere-Ocean General Circulation Models (AOGCMs) which are utilised to understand the dynamics of the physical components of the climate system (Flato et al., 2013).

Interactive carbon cycles and dynamically changing vegetation have been recognised as important processes in the earth system (Cox et al., 2000; Ciais et al., 2013). Consequently, more recent developments have seen AOGCMs extended to include biogeochemical cycles, most often the carbon cycle, to form a new category of model, Earth System Models (ESMs). These state-of-the-art models are the most comprehensive tools for modelling past and future climate change in which biogeochemical feedbacks play an important role, and for studying biosphere-atmosphere feedbacks explicitly (Flato et al., 2013). However, whilst all ESMs by definition have a carbon cycle, not all have truly dynamic vegetation or a nitrogen cycle, fewer still have prognostic representations of fire or of the phosphorous cycle. These processes change vegetation cover and structure in response to changing climate and fire activity, and thus models which do not include them miss key biosphere responses and corresponding feedbacks to the climate system (Wramneby et al., 2010).

To take the first steps towards constructing an ESM with dynamic vegetation, anthropogenic influences and fire, we have combined an atmospheric chemistry-enabled AOGCM, EMAC (Jöckel et al., 2010; Pozzer et al., 2011; Jöckel et al., 2016), with a DGVM, LPJ-GUESS (Smith et al., 2001; Sitch et al., 2003; Smith et al., 2014), in a single modelling framework. LPJ-GUESS is a state-of-the-art DGVM which has been widely applied and extensively evaluated, and has, in different model versions, been extended to include many terrestrial processes and used in over 200 ISI-listed publications [1]. At the time of writing LPJ-GUESS is actively developed and there are on-going efforts to consolidate many previously independent innovations into the main model release. This combination of active development, broad range of included processes and the flexible modelling framework design of the LPJ-GUESS source code makes it a good choice to provide the land surface component of an ESM.

Furthermore, LPJ-GUESS has already been used both a global ESM, EC-Earth (Weiss et al., 2014; Alessandri et al., 2017), and a regional ESM, RCA-GUESS (Wramneby et al., 2010; Smith et al., 2011; Zhang et al., 2014). In both modelling systems, climate variables and daily soil moisture from the atmospheric component and its land surface scheme are aggregated over one

[1] see *http://iis4.nateko.lu.se/lpj-guess/LPJ-GUESS_bibliography.pdf* for an up-to-date list of publications featuring LPJ-GUESS

simulation day and provided to LPJ-GUESS (Weiss et al., 2014; Smith et al., 2011). In the EC-Earth framework, LPJ-GUESS provides only time-varying leaf area index (LAI) to the atmospheric component which initially only affected physiological resistance (Weiss et al., 2014). This link was recently extended to include effects on albedo, surface roughness length, soil water exploitable by roots and snow shading by vegetation (Alessandri et al., 2017). The land surface scheme in RCA-GUESS splits the gridcell surface into two tiles, one of forest and one herbaceous vegetation, and LPJ-GUESS is used to dynamically adjust the LAI within those tiles and relative fractional coverage of needle-leaved and broad-leaved trees in the forest tile. These LAI and fractional cover values affect albedo, surface roughness and heat fluxes in the land surface scheme (Smith et al., 2011).

In the work reported here we have adopted a broadly similar approach with regards to forcing LPJ-GUESS with daily aggregated climate fields from the atmospheric model, although daily soil moisture values are calculated by LPJ-GUESS and not the land surface. In the model version described here, LPJ-GUESS return LAI, vegetation cover fractions, canopy heights and net primary production to EMAC, which allows dynamic calculation of transpiration (by using the vegetation cover provided by LPJ-GUESS as opposed to prescribed vegetation cover) and of albedo and surface roughness (using newly added parameterisations). However, this information is not (thus far) used by the land surface scheme. In other words, although there is two-way information flow and calculation of land surface properties, the model is only effectively coupled in one direction. Enabling the effect of LPJ-GUESS's dynamic vegetation on the atmosphere (via the land surface scheme) is still under development and will be reported in a future publication (for preliminary results see Tost et al., 2018). The integration of LPJ-GUESS into EMAC is independent of the development of the EC-Earth and RCA-GUESS, but we believe that there are possible synergies in terms of future model development. Furthermore, we consider this parallel development to be complementary in terms of scientific applications, in particular the representation of atmospheric chemistry processes in EMAC allows study of land-atmosphere interactions mediated by trace gas exchanges.

EMAC (ECHAM/MESSy Atmospheric Chemistry) originally combined the ECHAM atmospheric GCM (Roeckner et al., 2006) with the Modular Earth Submodel System (MESSy) (Jöckel et al., 2005) framework and philosophy. The model has since been extended to include state-of-the-art atmospheric chemistry, a coupled ocean model with dynamic sea ice (Pozzer et al., 2011), ocean biogeochemistry (Kern, 2013), an alternative base model for the atmospheric circulation (Baumgaertner et al., 2016), regional downscaling via a two-way coupling (Kerkweg et al., 2018) with the COSMO weather forecast model (Baldauf et al., 2011) and a multitude of processes such as representations for aerosols, aerosol-radiation and aerosol-cloud (Tost, 2017) interactions and many more; all of which are integrated via the MESSy infrastructure.

By bringing together these two state-of-the-art modelling systems, our intent is to produce a fully-featured ESM which benefits from the continuous development of both communities. In addition to the broad range of applications possible for any ESM, the particular strength of EMAC with LPJ-GUESS vegetation will be applications studying interactions and feedbacks at the atmosphere-biosphere boundary, for example: the nitrogen cycle, trace gas emissions from fire, the atmospheric dynamics of reduced carbon including biogenic volatile organic compound emissions from vegetation and methane from fires, ozone

dynamics and the resulting damage to vegetation, and the effects of a wide spectrum of terrestrially emitted trace gases on cloud and aerosol formation and dynamics.

In this manuscript we describe and verify the first steps of our model integration work. Firstly we describe the coupling approach and the technical details of the implementation. Secondly we evaluate the vegetation state produced by LPJ-GUESS as a result of a one-way coupling whereby LPJ-GUESS is forced on-line by daily climate values calculated by EMAC. These results are compared to a suit of remotely-sensed terrestrial biosphere datasets and an expert-derived map of global vegetation cover. Results from the full bidirectional coupling will be reported in a future publication.

2 Model description

2.1 The EMAC modelling system

The ECHAM/MESSy Atmospheric Chemistry (EMAC) model is a numerical chemistry and climate simulation system that includes sub-models describing tropospheric and middle atmosphere processes and their interaction with oceans, land and human influences (Jöckel et al., 2010, 2016). The historical starting point for the EMAC model was the ECHAM5 atmospheric model (Roeckner et al., 2006), but the original code has now been fully 'modularised' using the second version of the Modular Earth Submodel System (MESSy2) (Jöckel et al., 2010) including a comprehensive, but highly flexible infrastructure to the point that only the dynamical core and the runtime loop remain from the original code. The physical processes and most of the infrastructure have been split into 'modules' in accordance with the MESSy philosophy whereby such modules can be further developed to improve existing process representations, new modules can be added to represent new processes or alternative process representations, for example parameterised atmospheric convection (Tost et al., 2006), and modules can be selected at run time. EMAC has been extensively used for scientific applications of atmospheric chemistry and chemistry climate interactions from the surface to the mesosphere[2].

2.2 The LPJ-GUESS DGVM (v4.0)

At its core LPJ-GUESS (Smith et al., 2001; Sitch et al., 2003; Smith et al., 2014) is a state-of-the-art DGVM featuring a comparatively detailed individual based model of vegetation dynamics. These dynamics are simulated as the emergent outcome of growth and competition for light, space and soil resources among woody plant individuals and a herbaceous understorey in each of a number of replicate patches representing 'random samples' of each simulated locality or grid cell. Multiple patches are simulated to account for the distribution within a landscape representative of the grid cell as a whole of vegetation stands differing in their histories of disturbance and stand development (succession). The simulated plants are classified into one of a number of plant functional types (PFTs) discriminated by growth form, phenology, photosynthetic pathway (C_3 or C_4), bioclimatic limits for establishment and survival and, for woody PFTs, allometry and life history strategy (see Smith et al. (2014)

[2] see *http://www.messy-interface.org/* for an up-to-date list of publications featuring MESSy

for a description of the standard global PFTs). The simulations of this study were carried out in 'cohort mode,' in which, for woody PFTs, cohorts of individuals recruited in the same patch in a given year are identical, and are thus assumed to retain the same size and form as they grow.

Primary production and plant growth follow the approach of LPJ-DGVM (Sitch et al., 2003), and from version 3.0 onwards (we are using v4.0 here) LPJ-GUESS includes an additional nitrogen limitation on photosynthesis (Smith et al., 2014). Canopy fluxes of carbon dioxide and water vapour are calculated by a coupled photosynthesis and stomatal conductance scheme based on the approach of BIOME3 (Haxeltine and Prentice, 1996). The net primary production (NPP) accrued by an average individual plant each simulation year is allocated to leaves, fine roots and, for woody PFTs, sapwood, following a set of prescribed allometric relationships for each PFT, resulting in biomass, height and diameter growth (Sitch et al., 2003). Population dynamics (recruitment and mortality) are represented as stochastic processes, influenced by current resource status, demography and the life history characteristics of each PFT (Hickler et al., 2004, 2012). Forest stand destroying disturbances (such as wind throw and pest attacks) are simulated as a stochastic process, affecting individual patches with an expectation of 0.01 yr^{-1}. Litter arising from phenological turnover, mortality and disturbances enters the soil decomposition cycle. As of v3.0, decomposition of litter and soil organic matter (SOM) pools follows the CENTURY scheme as described in Smith et al. (2014). Biogenic volatile organic compounds (BVOCs) are emitted from vegetation depending on vegetation type, leaf temperature, atmospheric CO_2 concentration and carbon assimilation (Arneth et al., 2007a, b). Soil hydrology follows Gerten et al. (2004).

Photosynthesis, respiration and hydrological processes operate on a daily time step and require daily temperature, precipitation and incident short wave radiation. However, monthly climate data may be provided, in which case the model interpolates daily values from the monthly values. In these circumstances, the number of precipitation days in the monthly periods may also be provided to disaggregate total precipitation into distinct rain events. In the case of unmanaged natural vegetation (as simulated here), vegetation dynamics (such as establishment and mortality), disturbance, turnover of plant tissues and turnover between litter pools, and allocation of carbon and nitrogen to plant organs all occur on an annual basis.

The GlobFIRM fire model (Thonicke et al., 2001) is included in LPJ-GUESS. It is a simple model which simulates wildfires based on soil moisture (as a proxy for fuel moisture) and a minimum fuel (litter) threshold for burning. Other fire models of greater complexity have been used with LPJ-GUESS: SPITFIRE (Lehsten et al., 2009; Thonicke et al., 2010; Rabin et al., 2017), SIMFIRE (Knorr et al., 2016) and SIMFIRE-BLAZE (Rabin et al., 2017). Whilst these models are not currently in the main LPJ-GUESS code version used here, integration efforts are underway and it is is anticipated that they will be available soon in the main LPJ-GUESS version and subsequently in EMAC. Similarly, a representation of tundra, arctic wetlands and permafrost has been developed within a separate branch of LPJ-GUESS (Miller and Smith, 2012) which is now being re-integrated into the main model version. A human land use and agricultural framework (Lindeskog et al., 2013) is included in LPJ-GUESS v4.0 although it is not enabled in this study.

2.3 Overview of coupling implementation

The coupling strategy employed here was to modify LPJ-GUESS such that it provides its functionality via a new submodel in the MESSy framework. An important design priority was to maintain the integrity of the LPJ-GUESS source code by performing only minimal modifications and additions, in order to facilitate straightforward synchronising with the main LPJ-GUESS trunk version in the future. This approach was successful, with only minor changes made to LPJ-GUESS infrastructure code and no changes to the scientific modules. Three new functions were implemented to exchange information between LPJ-GUESS and MESSy. All these changes were implemented such that LPJ-GUESS can still be compiled outside EMAC and run as a stand-alone model. Within EMAC, the LPJ-GUESS code is compiled into a single library file and the three new functions are called by the new VEG submodel implemented in MESSy. The creation of a single library was necessary (as opposed to direct function calls) because LPJ-GUESS is written in *C++* whereas EMAC is written in *FORTRAN*. For more details see Appendix A.

To provide appropriate climate forcing for LPJ-GUESS, EMAC calculates the daily mean 2 m temperature, daily mean net downwards shortwave radiation and the total daily precipitation at the end of the simulation day and provided it to LPJ-GUESS. Atmospheric CO2 concentration and nitrogen deposition are also provided on a daily basis from EMAC to LPJ-GUESS. Thus the LPJ-GUESS land-surface state is forced completely by the EMAC atmospheric state.

In turn, LPJ-GUESS provides fractional vegetation cover, leaf area index, daily net primary productivity and average height of each PFT to EMAC. Parameterisations for determining albedo and roughness length are implemented in EMAC, however they are not enabled in the simulations presented here. Thus, we are demonstrating only a one-way coupling where the land surface state does not affect the atmospheric state. The boundary conditions for the atmospheric model (in particular the surface energy and water fluxes) come from the pre-existing land surface representation.

The coupling strategy is to tighten the coupling between LPJ-GUESS and EMAC in well-defined, consecutive steps and to assess the effects of one model on the other in a step-wise and logical manner. Here we report the effect of EMAC climate on LPJ-GUESS. The next step is to enable the albedo and roughness length schemes and to use the vegetation and forest fractions (which are used in the standard land surface scheme to determine the hydrological fluxes) to form a bidirectional coupling of interactive vegetation and climate. The work is underway (Tost et al., 2018) and will be presented in a future publication.

Future planned development steps are to enable land use and agriculture in LPJ-GUESS within EMAC, to include a more process-based representation of fire and include the relevant emissions, to fully replace the soil-vegetation part of the hydrological cycle in EMAC with that in LPJ-GUESS and to use LPJ-GUESS to close the land surface energy balance. When completed, these developments will extend the EMAC model into a full Earth system model including atmosphere (ECHAM5) with full chemistry (see Jöckel et al., 2010), vegetation and land surface processes (LPJ-GUESS) and an ocean component (MPIOM)

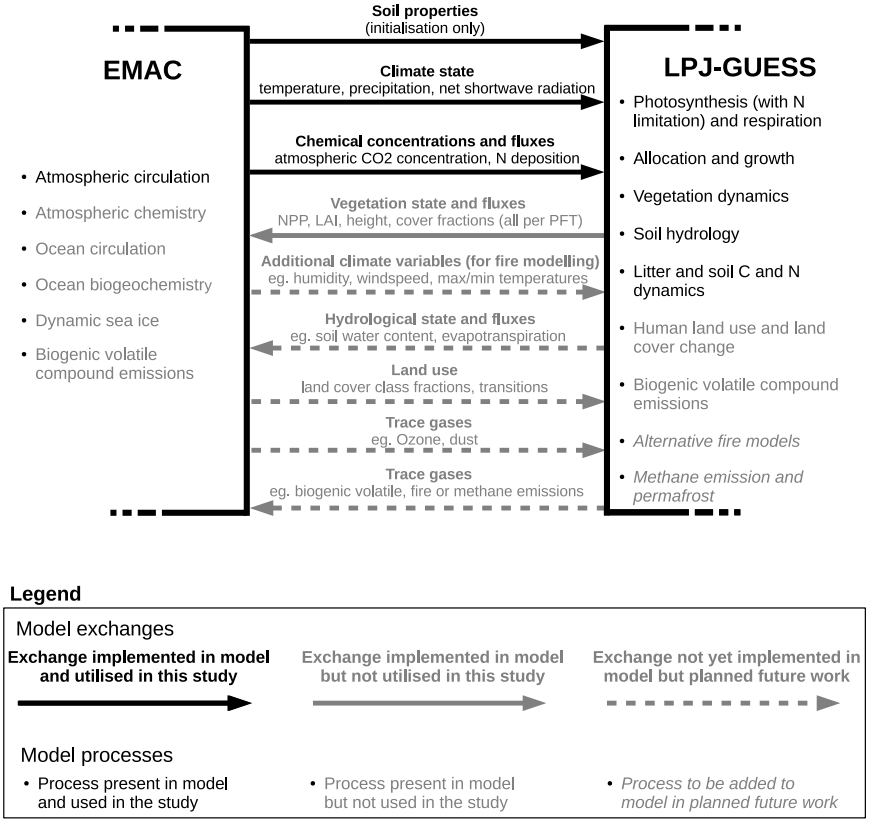

Figure 1. The main processes and exchanges in the coupled model framework. Processes/exchanges with normal black text/black solid arrows are included in the framework and used in the simulations presented here; processes/exchanges with normal grey text/grey solid arrows are included in the framework but not used in the simulations presented here; and processes/exchanges with italic grey text/grey dotted arrows are not included in the framework but planned in future work. All exchanges happen on a daily basis, except for soil properties which happen only during the initialisation phase.

(see Pozzer et al., 2011) with ocean biogeochemistry (see Kern, 2013). The process and exchanges currently included in the modelling framework, as well as planned future additions, are shown in Fig 1.

3 Simulation setup

In the coupled model, the vegetation produced by LPJ-GUESS within EMAC will be directly sensitive to biases in the climate produced by EMAC. It is well-known that these biases are dependent on spatial resolution; see Roeckner et al. (2006) for a study of the biases at different resolutions in ECHAM5 (the GCM upon which EMAC was original based). Whilst it is not within the scope of this study to perform a detailed analysis of the biases in EMAC or their dependence on spatial resolution, the impact of the horizontal spatial resolution of the atmospheric simulation on the vegetation simulation is relevant. To this end we

performed two simulations for this evaluation, here denoted *T42* and *T63*, which used T42 and T63 spectral resolutions respectively, but were otherwise identical. The applied EMAC model setup comprised the submodels for radiation (Dietmüller et al., 2016), clouds and convection, surface processes (see Jöckel et al., 2016), and 31 vertical hybrid pressure levels up to 10.0 hPa, representing a typical climate simulation. Note that for reasons of computational burden, the atmospheric chemistry calculations of which EMAC is capable were not activated in these simulations. The model was driven by constant solar (present day) conditions, with prescribed climatological sea surface temperatures (AMIP II Taylor et al., 2000), including an annual cycle. CO_2 was constant and maintained at a level of 367 ppm throughout the whole simulation. Throughout both the simulations, LPJ-GUESS was driven exclusively by climate variables from EMAC, at no point were external climate datasets used.

To aid the interpretation of the EMAC simulations, we also performed an 'offline' LPJ-GUESS simulation using observed climate data from the CRUNCEP bias-corrected, re-analysis dataset (Wei et al., 2014). The simulation was performed using exactly the same code and parameter settings as the EMAC *T42* and *T63* simulations, but code was compiled as a stand-alone model. The atmopsheric CO_2 concentration and nitrogen deposition follow Smith et al. (2014) and the simulation is referred to as the *CRUNCEP* simulation.

The LPJ-GUESS configuration contained 11 plant functional types (needle-and broad-leaved, deciduous and evergreen trees, as well as two types of grass as described in Smith et al. (2014)) and for each gridcell 50 replicate patches were simulated simulated and averaged to account for model stochasticity. Nitrogen deposition rates were prescribed using data from Lamarque et al. (2013) for the decade 1850-1859 throughout the *T42* and *T63* simulations. The degree of nitrogen limitation experienced by the vegetation in the simulations (quantified by the ratio of nitrogen limited to non-nitrogen limited photosythetic rates) is shown in Fig C1, which shows that pre-industrial nitrogen deposition does not result in additional nitrogen limitation. However, in future work, temporally-appropriate nitrogen deposition data will be used.

The model simulation duration was dictated by the need to spin-up the LPJ-GUESS vegetation into equilibrium. Here we followed the standard LPJ-GUESS procedure of starting with 'bare ground', ie. no vegetation and no C or N in the soil and litter pools, and running for approximately 500 years to allow the vegetation to reach equilibrium. Having no plant available N present in the soil at the start of the simulation would inhibit and distort vegetation growth if N limitation was enabled. To overcome this, we follow the standard protocol and run LPJ-GUESS for 100 years without N limitation but with normal N deposition to build up the N pools. After 100 years there is sufficient N in the pools, but the vegetation is inconsistent with the desired state as it has been growing without N limitation. Therefore, the vegetation is removed (and the C and N put into the litter pools), and the vegetation is allowed to regrow, this time with N limitation enabled, for a further 400 years. For the *T42* and *T63* simulations, the last 50 years of this 500 year simulation were averaged to produce the plots shown here. At that time, no significant trends in PFT extension and PFT height were obvious, but the vegetation shows interannual variability as expected. In the *CRUNCEP* simulation, the first 30 years (1901-1930) were repeated to provide climate data for a 500 years spinup, and then a further 113 years (1901-2013) were simulated using CRUNCEP data. The plots presented here show model

output averaged over the years 1981-2010.

4 Model evaluation

As LPJ-GUESS has been evaluated in detail in previous work, for example, net primary production (e.g. Zaehle et al., 2005; Hickler et al., 2006), modelled potential natural vegetation (Hickler et al., 2006; Smith et al., 2014), stand-scale and continental-scale evapotranspiration (AET) and runoff (Gerten et al., 2004), vegetation greening trends in high northern latitudes (Lucht et al., 2002) and the African Sahel (Hickler et al., 2005), stand-scale leaf area index (LAI) and gross primary productivity (GPP; Arneth et al., 2007a), forest stand structure and development (Smith et al., 2001, 2014; Hickler et al., 2004), global net ecosystem exchange (NEE) variability (Ahlström et al., 2012, 2015) and CO_2 fertilisation experiments (e.g. Hickler et al., 2008; Zaehle et al., 2014; Medlyn et al., 2015), it is beyond the scope of this work to perform a full model evaluation and propose improvements for the dynamic vegetation model. Instead we evaluated the coupled model setup to consider how LPJ-GUESS responds when EMAC climate is used as the forcing data and to investigate any biases in the vegetation produced. For this we used an expert-derived Potential Natural Vegetation (PNV) map and using remotely-sensed data sets of tree cover (Dimiceli et al., 2015), canopy height (Simard et al., 2011) and biomass (Avitabile et al., 2016; Thurner et al., 2014).

To provide an overall summary metric of data-model agreement across the relevant spatial domain, the Normalised Mean Error (NME) is presented following the prescription and recommendations in Kelley et al. (2013). These summary metrics are not meant to demonstrate a particular level agreement better than some arbitrary threshold. Nor are they mean for strict evaluation or comparison to other models, since here we evaluating only the first milestone of model development and so the model is known to be incomplete (particularly with regard to human land use) and no tuning has been performed. They are included to quantitively evaluate the differences between models runs at difference resolutions and for assessing the effect of human land use via a land cover correction factor (see below).

It should be noted that the NME is rather different from a coefficient of correlation or a coefficient of determination. It does not attempt to derive a correlation but instead sums the differences between the model and the observation. It can be thought of as quantifying the deviation from the one-to-one line of perfect data-model agreement, rather than the deviation from a line of best fit. This means that is a rather direct and unforgiving metric, since every deviation of the model from the data is penalised (uncertainty is not included) and there is no possibility for the line of best fit to move to compensate for systematic biases. It also means the values are interpreted in the opposite direction to a correlation coefficient; an NME score of zero implies perfect agreement between observation and model, whereas an r^2 of zero would imply no correlation between the two. By the normalisation implicit in the method, using the mean value of the observations in place of the model gives an NME of unity.

At this stage of model development we do not seek to precisely simulate the vegetation state of a particular year or period. Our atmospheric simulations are not nudged by meteorological data, but rather an unconstrained simulation based on a single year of SSTs, so they do not correspond to a particular calendar period. Furthermore we prescribe a fixed atmospheric CO_2 concentration. Instead, our goal with this evaluation is to perform steady state simulations where the climate and CO_2 forcing are constant and correspond approximately to conditions in the recent past. Thus, after 500 years of simulation, we can compare the equilibrium vegetation to satellite products based on observations in the early 2000s. Whilst we can't expect perfect agreement since (among other reasons) this is not a full transient simulation, the simulations should be sufficient to check if the model coupling is working as intended, and to gain some insight into biases that may be present when LPJ-GUESS is forced using EMAC climate. Furthermore, it should be noted that the tree cover and biomass datasets reflect the biosphere as observed in the previous decade or so, and therefore inherently contains the considerable effect of human land use. This results in a conceptual mismatch between the PNV as simulated by LPJ-GUESS and the observed biosphere state which is relevant when considering these comparisons. To quantify this effect, NME scores including a land use correction (see Appendix E for details) for these datasets are also included in Section 4.5.

Whilst it is not within the scope of this work to evaluate the biases of climate state produced by EMAC, knowledge of these biases is very useful for disentangling the causes of model-data disagreement in the simulated vegetation. To this end, we include bias plots of seasonal and annual biases in surface temperature, precipitation and net (plant-available) short wave radiation of the EMAC *T42* and *T63* climate with respect to the CRUNCEP bias-corrected, re-analysis climate dataset in Appendix B.

4.1 Biomes

The simulated Leaf Area Index (LAI) was used to classify the vegetation cover into eight "megabiome" types following Forrest et al. (2015). The broad vegetation categories give an overview of the vegetation structure and functioning at a level of detail relevant for studying interactions between the land surface and the atmosphere. These simulations results were compared to an expert-derived potential natural vegetation (PNV) map (Haxeltine and Prentice, 1996) classified into equivalent categories (Smith et al., 2014; Forrest et al., 2015) which was regridded using a largest area fraction algorithm to the spatial resolution of the simulations. It should be borne in mind that there are various sources of uncertainty affecting the classification of biomes in both the data and the model output, such as the somewhat subjective LAI threshold applied to the model data and the inherently subjective nature of expert classification. However, these uncertainties are to some extent minimised by the choice of broad megabiomes (see Forrest et al. (2015) for further discussion) and so, despite this lack of quantitative rigour, such classifications still provide a useful visual method for comparing vegetation cover.

The simulations reproduce the global patterns of vegetation cover well (2), although some regional discrepancies are visible. The most obvious mismatch between all the simulations and the reconstructed megabiomes is the underestimation of the abundance of vegetation in the high northern latitudes. The tendency is relatively small in the *CRUNCEP* simulation, but

larger for the EMAC simulations. The higher resolution *T63* simulation is better than the *T42*, as it shows a greater tundra and boreal forest extent. Therefore, this mismatch can be attributed to a high-latitude growing season low temperature and low plant available radiation bias in the EMAC climate (Figs B2 and B3) at low resolution, which is somewhat mitigated at higher resolution due to a better representation of the synoptic scale systems in T63 (Roeckner et al., 2006).

The extent of the temperate forest of the east coasts of the USA and China was underestimated in the simulations using the EMAC climate, which is not seen in the *CRUNCEP* simulations. Inspection of the climate bias plots (Figs B1, B2, B3) shows that this can be attributed to a negative bias in precipitation in the southern areas, and negative bias in the plant available radiation in the northern area of coastal China. Large negative precipitation biases reduce the extent of the tropical forest in Indonesia and Papua New Guinea, and in the north-east coast of South America (not seen in the *CRUNCEP* simulations). In central Africa and the interior of Brazil, the extent of the tropical forests is also much reduced compared to *CRUNCEP*. However, in this case the reasons are not immediately clear from examination of the bias plots, although some seasonal biases in precipitation and plant available radiation are not clearly apparent. The extent of the Savanna and Dry Woodlands vegetation type is also under-simulated in Australia and eastern Africa as a result of a negative precipitation bias, although this extent is also not well represented in the *CRUNCEP* simulation. The extent of the Sahara Desert is also underestimated in the EMAC and *CRUNCEP* simulations, as some areas grow sufficient grass cover to be classified as short grasslands. As this is present in the *CRUNCEP* simulation, it is not related to a climate biases, but rather the over-simulation of grasses in very arid regions by LPJ-GUESS.

Given that the *T42* and *T63* results are broadly similar, for brevity of the presentation the subsequent *T42* results will be omitted from the subsequent spatial benchmarks, although the *T42* summary metric results will be tabulated and discussed.

4.2 Tree cover

The collection 6 of the MOD44B MODIS tree cover (Dimiceli et al., 2015) was averaged between 2000 and 2015, interpolated to the simulation resolutions using conservative remapping (Jones, 1999; CDO, 2018) and then compared to the simulated tree cover. The combined model produced reasonable global tree cover patterns as would be expected by a state-of-the-art DGVM (Fig. 3). However, regional differences are clearly visible which can be attributed to three main sources. The most prominent of these are due to the fact that the simulation is of PNV (ie no human land use processes are included in the simulation) where the observations are of the current state of the planet and therefore include the impact human land use. This conceptual mismatch in the comparison can reasonably account for the large over-estimations of tree cover in Europe, China and temperate North America. The second possible reason for discrepancies in modelled tree cover compared to observed tree cover is climate biases in the EMAC-produced climate. For example, this is apparent in the underestimation of tree cover on the north-east coast of South America, as already indicated in the biome plots (Fig. 2), which is clearly the result of a large negative precipitation bias in the region (see B1). A final source of disagreement is due to the inevitable imperfect process representations in LPJ-GUESS.

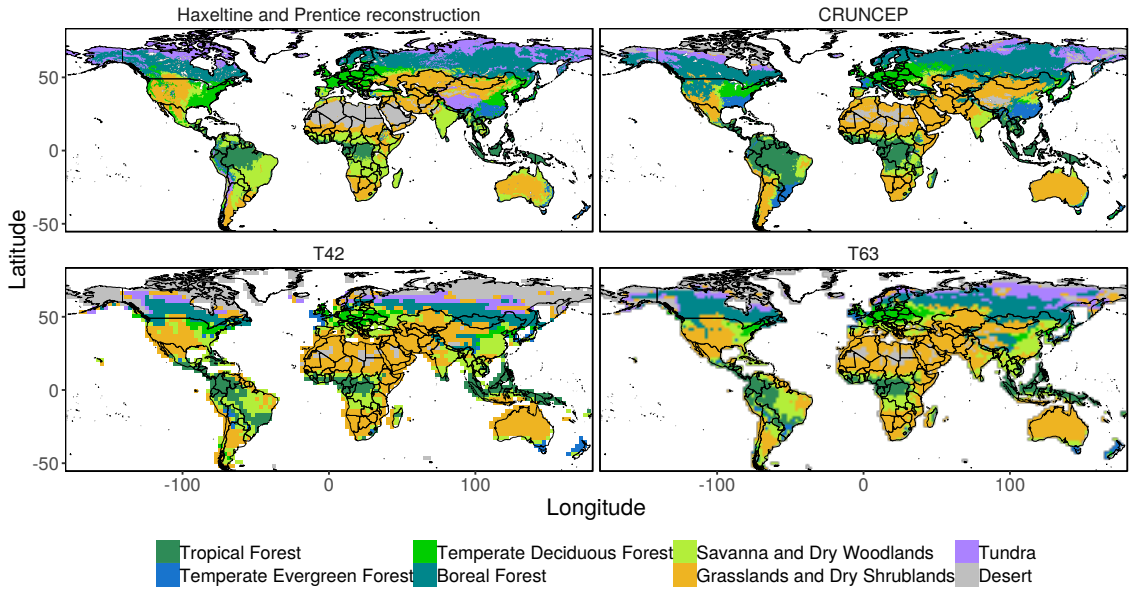

Figure 2. Distribution of PNV megabiomes simulated by LPJ-GUESS within EMAC (*T42* and *T63*) and using observed climate data (*CRUNCEP*) compared to an expert-derived PNV map.

This is exemplified by the over-estimation of tree cover north of the central African tropical forest in both the EMAC and CRUNCEP forced simulations.

4.3 Biomass

Standing biomass is a key state variable in ESM and DGVMs as it is connected to productivity, carbon sequestration, evapotranspiration, vegetation cover, canopy height and other critical processes and variables which are relevant to vegetation functioning and land-atmosphere exchanges. As such, it is a useful quantity for evaluating DGVM/ESM performance. We combined two biomass datasets, one tropical (Avitabile et al., 2016) and one northern temperate and boreal (Thurner et al., 2014), by aggregating them to approximately 25 km resolution, interpolating them to the simulation resolutions using conservative remapping and then finally joining the maps (taking the average where they overlapped) to produce a nearly global map of standing biomass. Note that no data (non-forested) pixels in the original Thurner et al. (2014) dataset were set to zero to ensure consistency after the averaging procedure with the Avitabile et al. (2016) data.

The coupled model simulates well the global patterns of biomass (Fig 4), but it does not capture the very high biomass observed in the tropical forests. This underestimation is seen to a lesser extent in the CRUNCEP simulation. The different degrees of underestimation of tropical biomass by the CRUNCEP and EMAC *T63* simulations cannot be explained by the different nitrogen deposition forcing data (C1), however negative seasonal biases in plant available radiation and precipitation

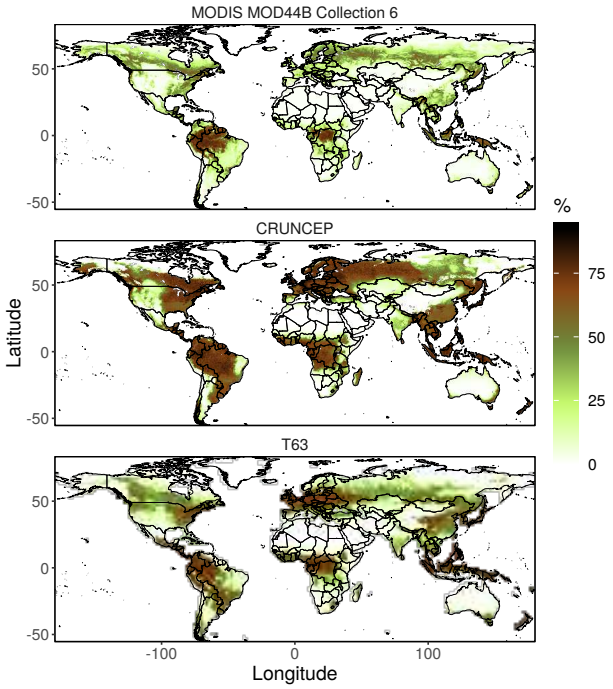

(a)

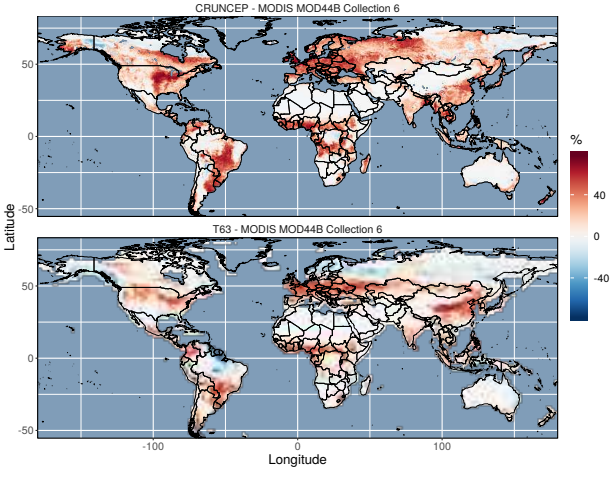

(b)

Figure 3. Comparison of tree cover from the *T63* (EMAC climate) and *CRUNCEP* (observed climate) simulations with observed tree cover from Dimiceli et al. (2015), a) absolute values and b) the difference between simulations minus observations.

are visible in these regions (Figs B1 and B3). It also underestimates biomass as in the north-east South America and south-east Asia, as would be expected from the biome and tree cover plots (Figs 2 and 3). There is also an over-estimation (small in

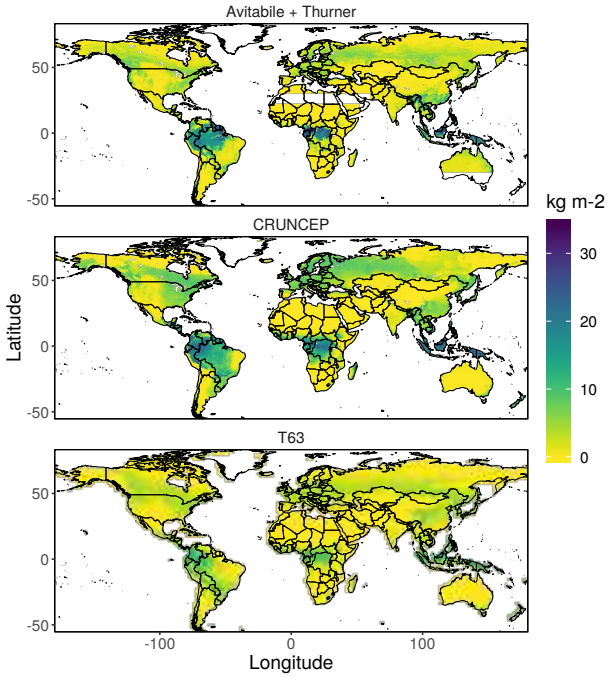

(a)

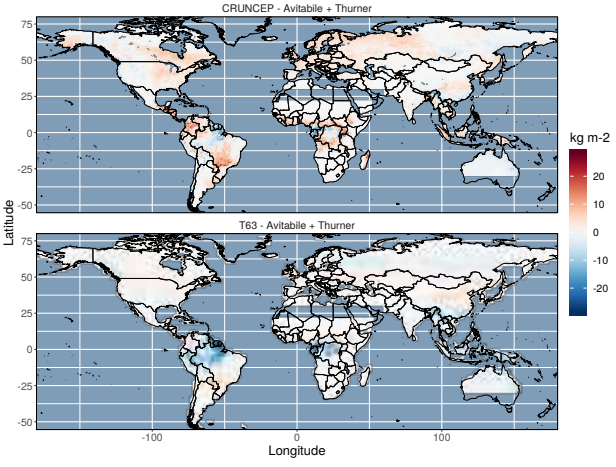

(b)

Figure 4. Comparison of biomass from the *T63* (EMAC climate) and *CRUNCEP* (observed climate) simulations with observed biomass from Avitabile et al. (2016) and Thurner et al. (2014), a) absolute values and b) the difference between simulations minus observation. Note that neither the Avitabile et al. (2016) nor the Thurner et al. (2014) biomass dataset provide biomass for a band across the Sahara, so no data are plotted there.

magnitude but large as a relative fraction) of biomass in Europe and China, most likely due to human land use.

4.4 Canopy height

In the case of a bidirectional coupling, the simulated canopy height will have a direct effect on atmospheric circulation through roughness length. To evaluate simulated canopy height, a 1 km tree canopy height map (Simard et al., 2011) was first aggregated to 10 km resolution by simple averaging (excluding no data values) and then interpolated to the simulation resolution using conservative remapping. Comparison of these data with simulated canopy height (calculated from individual tree height, see Appendix D) revealed that the coupled model simulates global distributions of canopy height reasonably well (Fig 5), but systematically underestimates tree height in highly forested areas. The *CRUNCEP* simulation shows a similar tendency to underestimate canopy height in some regions, indicating that is systemic behaviour in the current LPJ-GUESS parameterisation. In light of the biomass results in Section 4.3 where biomass is generally underestimated, it may be that the disturbance interval is too frequent, which does not allow sufficient time for biomass and canopy height to build up to realistic levels. Adjusting the disturbance frequency may therefore offer a solution. Another possible cause is the current maximum crown area of trees at 50 m^2 in LPJ-GUESS, which is rather low for tropical trees, and may result in an under-weighting of the contribution of mature individuals to canopy height (see Appendix D). In contrast, the simulations tended to overestimate canopy height in arid areas (both *T63* and *CRUNCEP*). This may be attributed to the lack of shrub PFTs and/or a low competitiveness of grass PFTs vs tree PFTs, possibly due to an under-estimation of fire frequency. In summary, the pattern of global canopy height is acceptable, but it may be appropriate to adjust the parameterisation in LPJ-GUESS to better reproduce global canopy height in the EMAC framework.

4.5 Summary metrics

The NME scores for both the *T63* and *T42* simulations are presented in Table 1 (lower is better). In the case of tree cover and biomass, the results are also presented with a land use correction (LUC) factor (see Appendix E). Applying the LUC has a marked improvement on the NME scores for tree cover, implying that some of the discrepancies seen between simulation and observation apparent in Fig 3 and 4 are indeed due to human land use. This also suggests that applying a land use scheme or correction will be important when enabling feedbacks from the land surface to the atmosphere in the future. For biomass the results are not so clear cut, as including the land use corrections worsens agreement, particularly for the *T42* simulation. This can be understood in the context of Fig 4 which shows that the combined model underestimates biomass, and so it can be expected that further reducing the biomass (through the land use correction) will worsen agreement. This indicates the importance of including land use effects in a consistent and realistic way in the coupled model, and that improved simulation of biomass is also critical due its status as a key state variable in the land surface representation. In particular, the average global patch-destroying disturbance rate of 0.01 yr-1 could be re-evaluated and rather simplistic mortality and tissue turnover rates

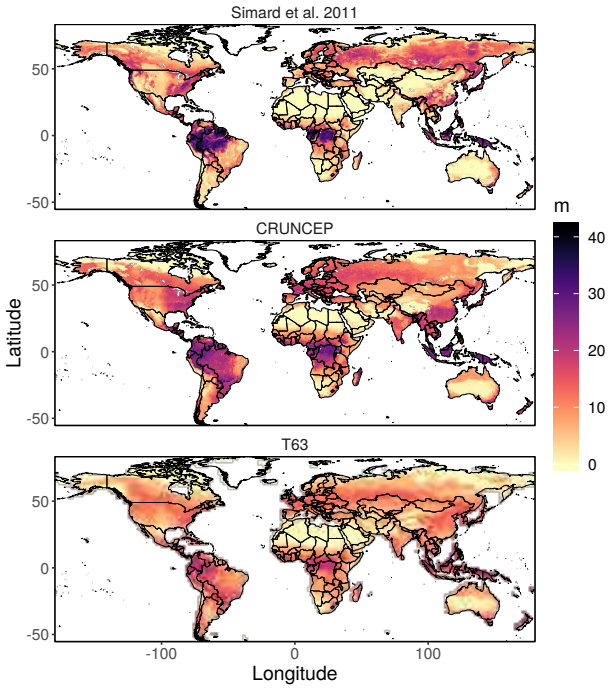

(a)

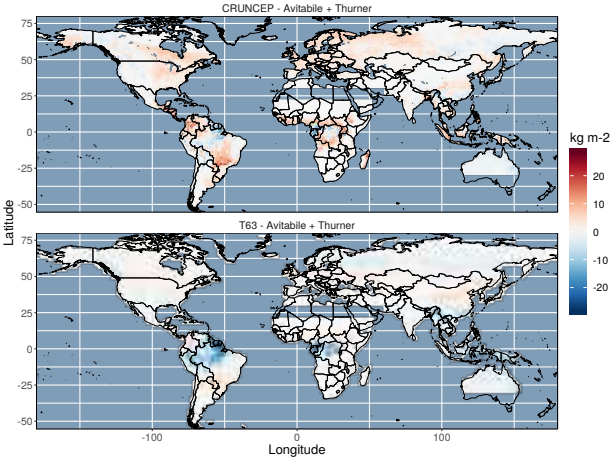

(b)

Figure 5. Comparison of canopy height from the *T63* (EMAC climate) and CRUNCEP (observed climate) simulations with observed canopy height from Simard et al. (2011), a) absolute values and b) the difference between simulations minus observation.

could be further developed in LPJ-GUESS.

Table 1. NME scores for the vegetation profuced by the *T42*, *T63* and *CRUNCEP* simulations compared to three remotely-sensed global datasets both with and without a LUC (Land Use Correction) where applicable. Note that lower scores imply better agreement between simulation and observation.

	without LUC			with LUC		
Dataset	*T42*	*T63*	*CRUNCEP*	*T42*	*T63*	*CRUNCEP*
Tree cover (Dimiceli et al., 2015)	0.94	0.85	1.1	0.81	0.69	0.62
Biomass (Avitabile et al., 2016; Thurner et al., 2014)	0.7	0.8	0.76	0.67	0.7	0.56
Canopy height (Simard et al., 2011)	n/a	n/a	n/a	0.96	0.81	0.77

The canopy height data was produced in such a way that no land use correction is necessary.

For the coupled simulations, increasing spatial resolution also improves the agreement between simulations and observation. This indicates that increased spatial resolution improves the representation of the climate in EMAC which in turn tangibly improves the vegetation simulated by LPJ-GUESS. This is particularly noteworthy as conducting benchmarking at higher resolutions is more rigorous and would generally be expected to result in lower benchmark scores. This can be understood mathematically as a consequence of a larger degree of spatial aggregation (of both the evaluation data and the model input data) at coarser resolutions leading to more homogenised values and therefore more agreement. While the result that the resolution of the atmospheric simulation has such a significant effect on the vegetation is not surprising in itself, it does highlight that when considering the bidirectionally coupled model with dynamic (as opposed to prescribed) vegetation, thorough investigation must be made of the effect of the resolution of the atmospheric model on both model components, particularly considering feedbacks between them.

5 Conclusions

Here we have reported the first steps towards to producing a new atmospheric-chemistry enabled ESM by combining an atmospheric-chemistry enabled AOGCM with a DGVM. The technical coupling work is now complete and has been achieved in a manner which respects both the integrity and philosophy of the two modelling frameworks, and will therefore allow relatively straightforward updates to both components.

Results from one-way coupled simulations (in which climate information generated by EMAC is used to force LPJ-GUESS but no land-surface information is relayed back to EMAC) showed that the vegetation patterns produced from EMAC climate are reasonable on a global scale. However some regional deviations from the observed vegetation are apparent. Some of these are due to the simple fact that in this configuration LPJ-GUESS produces PNV (potential natural vegetation with no human impacts) while the observed vegetation implicitly includes human impact. This effect was confirmed by performing a correction to account for human land use which improved agreement between simulation and observation. Human land use can be included in future model versions by utilising the recently developed crop and managed land module in LPJ-GUESS (Lindeskog et al.,

2013), the use of which should mitigate these issues to a large extent.

A second class of deviations is due to biases in the simulated climate, particularly precipitation biases. This is a more difficult problem to solve; improving climate simulations is the subject of much on-going research. However, it is clear that using higher spatial resolution mitigates climate biases which results in tangible improvements in the simulated vegetation. Furthermore, using dynamically simulated land surface boundary conditions (in this case from LPJ-GUESS) in a bidirectionally coupled model will alter the atmospheric state and therefore the climate biases. This will be the subject of future studies.

Finally, there are some discrepancies arising as an inevitable consequence of the approximations, missing processes and parameter uncertainties inherent in a process-based model such as LPJ-GUESS. These may be reduced by on-going improvements occurring as LPJ-GUESS is further developed and refined. Given the rather rigorous requirements placed on a biosphere model when bidirectionally coupled to an atmospheric model, it may also be necessary to perform some focused model development work with the goal of improving vegetation functioning and structure so that key biophysical quantities (such as albedo and roughness length) are better simulated. However no simulation model is perfect, and some biases and imperfections are inevitable in any model component.

Whilst further work remains before the full ESM is completed, we have demonstrated that coupling LPJ-GUESS into the EMAC/MESSy modelling framework has been accomplished, and that LPJ-GUESS provides a suitable basis for an improved and dynamic representation of the land surface in EMAC. A future publication will present a two-way model coupling and investigate the effects of the atmosphere. Once the full coupling has been enabled and calibrated, the resulting model will be a unique tool for investigating atmosphere-biosphere interactions.

Code availability. The Modular Earth Submodel System (MESSy) is continuously further developed and applied by a consortium of institutions. The usage of MESSy and access to the source code is licensed to all affiliates of institutions which are members of the MESSy Consortium. Institutions can become a member of the MESSy Consortium by signing the MESSy Memorandum of Understanding. More information can be found on the MESSy Consortium Website (http://www.messy-interface.org). As the MESSy code is only available under license, no DOI is possible for MESSy code versions. However, the code for coupling to LPJ-GUESS used in this manuscript is already included in the next official MESSy version (v2.54), which will be released in the coming weeks.

LPJ-GUESS is used and developed world-wide, but development is managed and the code maintained at Department of Physical Geography and Ecosystem Science, Lund University, Sweden. Model code can be made available to collaborators on entering into a collaboration agreement with the acceptance of certain conditions. The MESSy-coupled version of LPJ-GUESS will be maintained as a derivative of LPJ-GUESS. Because access to LPJ-GUESS is also restricted, no DOI can be assigned to LPJ-GUESS versions. The specific code version used here to enable the MESSy coupling the LPJ-GUESS code in EMAC, code is archived on the LPJ-GUESS subversion server with tag

"_publications/MESSY_1.0_20180108" in the catalogue "MESSy". For more details and contact information please see the LPJ-GUESS website (http://web.nateko.lu.se/lpj-guess) or contact the corresponding author.

For review purposes, the code used here is available to the editor and reviewers via a password protected link on condition that the code is for review purposes only, it cannot be used for any other purposes and must be deleted afterwards.

Appendix A: Details of coupling implementation

The following modifications were made to the LPJ-GUESS code:

- Creation of three new functions to be called externally by the MESSy framework to: initialise an LPJ-GUESS simulation (or restart from a saved state if appropriate); perform one day of LPJ-GUESS simulation given one day of EMAC climate data and return the relevant data; and save the LPJ-GUESS state to disk. These key functions encapsulate the interactions between MESSy and LPJ-GUESS.
- Creation of a new input module (an instantiation of the LPJ-GUESS *C++* class `InputModule`) to handle model initialisation in the MESSy framework, and the inclusion of one extra member function of the `InputModule` class (to read the gridlist file) which was implemented as a dummy function in the other LPJ-GUESS input modules.
- Creation of one additional internal function to calculate the daily values to be handed back to EMAC (such as vegetation cover for a particular PFT).
- Inclusion of an additional output module to save model output useful for benchmarking.
- Minor modifications to the standard output module such that the MPI rank number of each process is added to the file output names allowing the output from each process to be stored in the same directory.
- Minor modifications to the standard LPJ-GUESS restart code to allow the MESSy restart cycle number to be added to the names of the state files to be saved or read by LPJ-GUESS.
- Removal of some of code for the LPJ-GUESS real-time visualisations which is incompatible with the MESSy framework.

No changes to the scientific modules were made, and the directory structure and compilation machinery were untouched. Wherever new code conflicted with the standard offline version, a preprocessor directive was used to ensure that the model still compiled in the standard way outside the MESSy framework. Thus the integrity of LPJ-GUESS was maintained so that updates from the LPJ-GUESS trunk version can be applied relatively easily and the code can still be compiled and run offline.

On the MESSy side, the `Makefile` has been modified to compile the complete LPJ-GUESS code into a single library file using `CMake`, which is LPJ-GUESS's native compilation machinery. This was necessary because LPJ-GUESS is written in *C++* whereas EMAC is written in *FORTRAN*. The LPJ-GUESS library is linked to the rest of the EMAC code with the standard linker of EMAC (also including a link to *C++* standard library). LPJ-GUESS provides functionality to new EMAC

submodel (VEG) with its individual submodel interface layer (see Jöckel et al., 2005), which is controlled by a namelist and invokes the above mentioned *C++* functions to communicate with LPJ-GUESS.

In the initialisation phase, the grid from EMAC is transferred into LPJ-GUESS. Note, that currently there is only a geographic decomposition induced by EMAC, which could lead to some processors not having a single land box and cause idle time for that specific CPU. In future an additional, individual decomposition of the land gridcells to optimise CPU balance is desired, which could make use of the *UniTrans* library developed within the ScalES project[3], which shall also be used for load balanced distribution of chemical gaseous reactions. However, currently the LPJ-GUESS code with its daily timestep consumes very little computing time compared to the climate calculations of EMAC.

In its interface layer, the VEG submodel accumulates the required input fields (daily temperature, precipitation, incoming solar radiation and atmospheric CO_2 concentration) for the vegetation and, depending on the time step length of the LPJ-GUESS code, triggers the call of the LPJ-GUESS routines using the *TIMER*-MESSy interface structure routines (see Jöckel et al., 2005).

The combined model uses the pre-existing restart facilities of the LPJ-GUESS code, such that when EMAC triggers a restart, a restart is triggered for LPJ-GUESS. When a simulation is continuing from a restart, a flag is sent to the LPJ-GUESS code and the restart files of LPJ-GUESS state are read in allowing a seamless, continuous simulation. This feature may also be used to start a simulation with already well established vegetation from LPJ-GUESS restart (state) files, potentially significant saving significant amounts of CPU time that would otherwise be required to spin up the vegetation (typically the order of 500 simulation years).

[3]https://www.dkrz.de/Klimaforschung/dkrz-und-klimaforschung/infraproj/scales/scales

Appendix B: EMAC climate biases

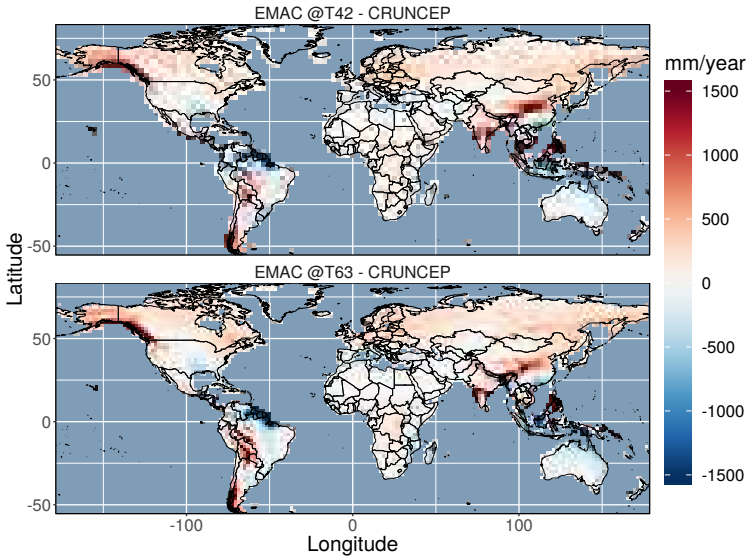

(a)

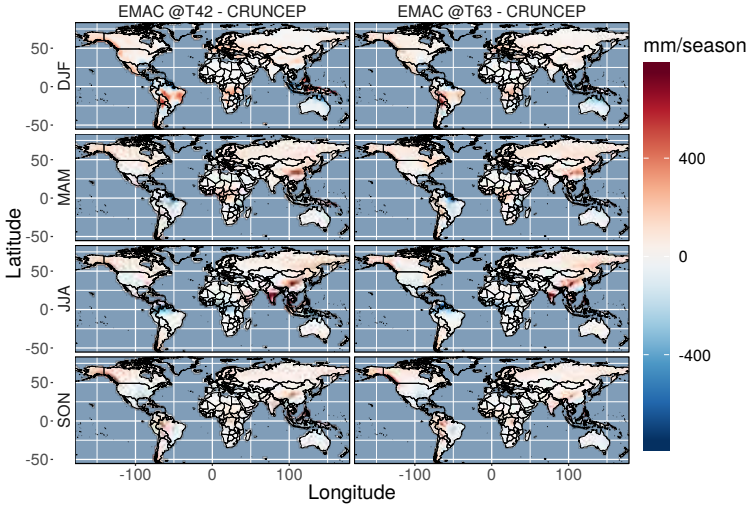

(b)

Figure B1. The a) mean annual precipitation bias and b) mean seasonal precipitation bias between the observed CRUNCEP dataset (1981-2010) and EMAC simulations (last 50 years of simulation). Note that ensure visibility of relatively low precipitations biases, the plotted values are capped at 750 mm/season and 1500 mm/year in the seasonal and annual plots, respectively.

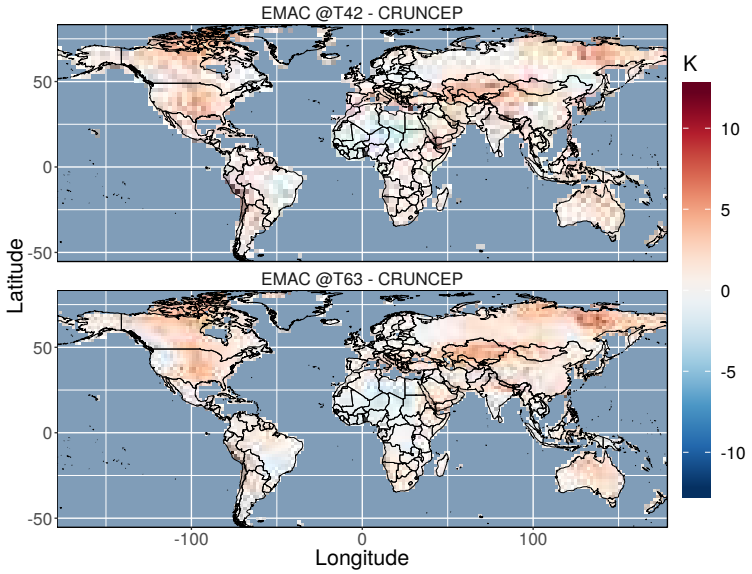

(a)

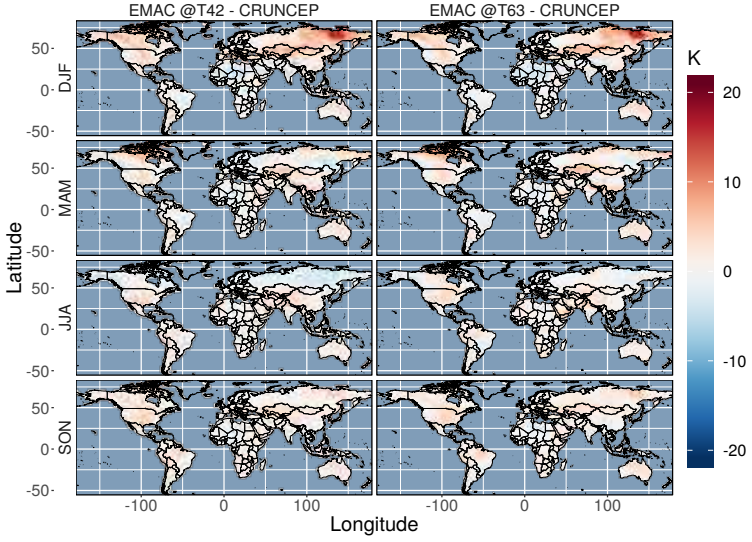

(b)

Figure B2. The a) mean annual temperature bias and b) mean seasonal temperature bias between the observed CRUNCEP dataset (1981-2010) and EMAC simulations (last 50 years of simulation).

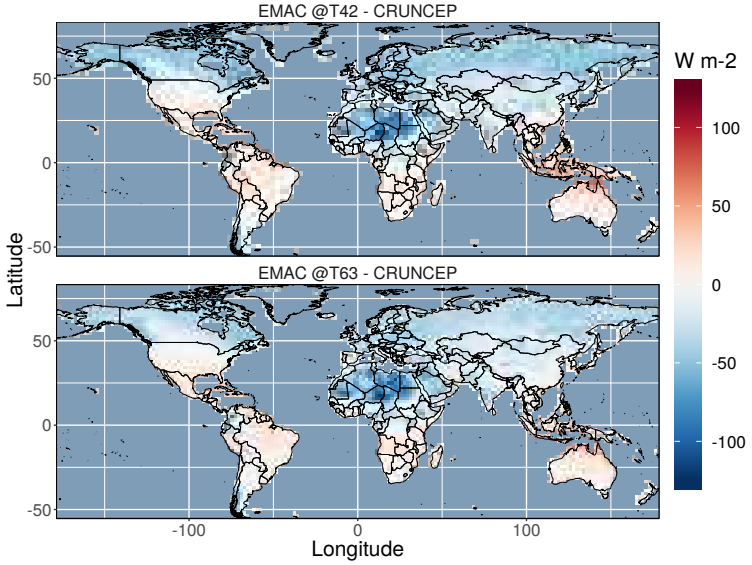

(a)

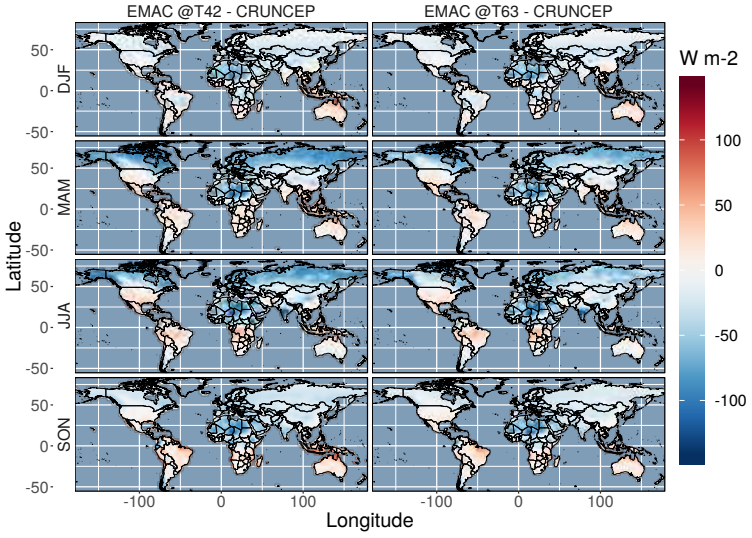

(b)

Figure B3. The a) mean annual net shortwave radiation bias and b) mean seasonal net shortwave radiation bias between the observed CRUNCEP (1981-2010) and EMAC simulations (last 50 years of simulation). Note that these plots compare shows the radiation available for vegetation in the CRUNCEP and EMAC forced LPJ-GUESS simulations, and consequently the gross shortwave radiation has been adjusted by different albedo values. The CRUNCEP radiation has been adjusted using the standard LPJ value of 0.17 applied (temporally and spatially invariant), and the EMAC radiation has been adjusted by the spatially and temporally varying albedo values in the land surface scheme.

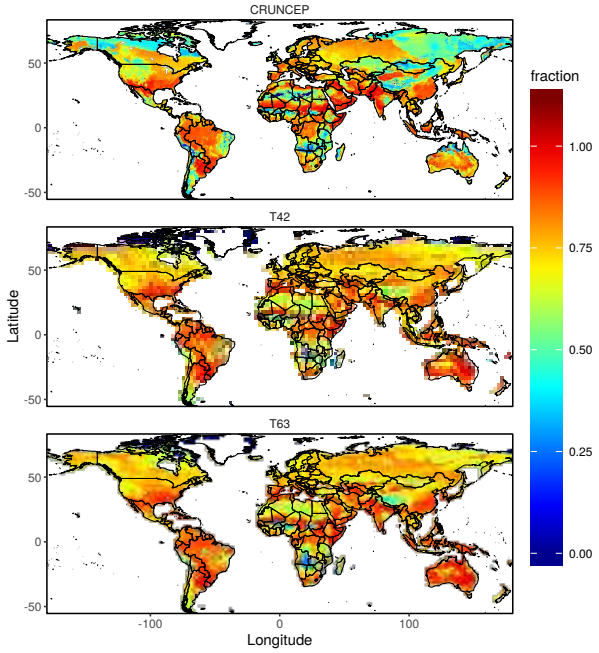

Figure C1. The ratio of nitrogen limited to nitrogen non-limited photosynthetic rates (weighted by leaf biomass) in all simulation runs.

Appendix C: Nitrogen limitation

Appendix D: Canopy height calculation

Canopy height of a patch was calculated from individual tree cohort heights by a simple algorithm that attempts to reconstruct top of canopy height as it would be viewed from above, for example by a satellite. It utilises the modelled quantity Foliar Projective Cover (FPC), which is the ground area covered by the crowns of trees of a cohort expressed as a fraction of the patch area. LPJ-GUESS allows limited overlapping of trees and hence the sum of tree cohort FPC can be greater than unity. In this case cohorts are selected in descending order of height until the sum of their FPC reaches 1, i.e. smaller cohorts are assumed to be under the taller cohorts and so do not contribute to top of canopy height. Cohorts smaller than 5 m don't contribute to canopy height as the remotely-sensed dataset does not include canopies lower than 5 m. Having selected the contributing tree cohorts, the canopy height is simply the FPC-weighted sum of the contributing cohort heights.

Appendix E: Land use correction

In order to correct the model output for 'missing' tree cover and biomass due to human land cover modification, a simple correction was derived from the Globcover2009 land cover product (Arino et al., 2012). For each simulated gridcell the fraction of naturally vegetated land pixels from the Globcover2009 product was calculated. This fraction was then used to scale the

model outputs of tree cover and biomass to give a simple, first order reduction based on remotely-sensed data. For these purposes, natural vegetated land cover was defined as classeswas defined by the following classes in the Globcover 2009 dataset:

- 40 Closed to open broadleaved evergreen or semi-deciduous forest
- 50 Closed broadleaved deciduous forest
- 60 Open broadleaved deciduous forest/woodland
- 70 Closed needleleaved evergreen forest
- 90 Open needleleaved deciduous or evergreen forest
- 100 Closed to open mixed broadleaved and needleleaved forest
- 110 Mosaic forest or shrubland/ grassland
- 120 Mosaic grassland/forest or shrubland
- 130 Closed to open (broadleaved or needleleaved, evergreen or deciduous) shrubland
- 140 Closed to open herbaceous vegetation (grassland, savannas or lichens/mosses)

Author contributions. HT and MF performed the model coupling. MF performed the simulations and analysis. All authors contributed to the overall model coupling strategy and to the manuscript.

Competing interests. The authors declare no competing interests.

Acknowledgements. Parts of this research were conducted using the supercomputer Mogon and/or advisory services offered by Johannes Gutenberg University Mainz (hpc.uni-mainz.de), which is a member of the AHRP (Alliance for High Performance Computing in Rhineland Palatinate, www.ahrp.info) and the Gauss Alliance e.V. Further development and the main simulations were performed using the LOEWE-CSC supercomputer at the High Performance Computing initiative. The authors gratefully acknowledge the computing time granted on the supercomputer Mogon at Johannes Gutenberg University Mainz (hpc.uni-mainz.de) and the LOEWE-CSC supercomputer at Goethe University Frankfurt (csc.uni-frankfurt.de).

The authors acknowledge the support of the MESSy core development team and are grateful for hints and discussions. Similarly, the authors recognise and appreciate the many improvements to LPJ-GUESS by the LPJ-GUESS development team which made this work possible, and thank the team (particularly Johan Nord) for their support.

References

Ahlström, A., Schurgers, G., Arneth, A., and Smith, B.: Robustness and uncertainty in terrestrial ecosystem carbon response to CMIP5 climate change projections, Environmental Research Letters, 7, 044 008, https://doi.org/10.1088/1748-9326/7/4/044008, http://stacks.iop.org/1748-9326/7/i=4/a=044008, 2012.

Ahlström, A., Raupach, M. R., Schurgers, G., Smith, B., Arneth, A., Jung, M., Reichstein, M., Canadell, J. G., Friedlingstein, P., Jain, A. K., Kato, E., Poulter, B., Sitch, S., Stocker, B. D., Viovy, N., Wang, Y. P., Wiltshire, A., Zaehle, S., and Zeng, N.: The dominant role of semi-arid ecosystems in the trend and variability of the land CO2 sink, Science, 348, 895–899, https://doi.org/10.1126/science.aaa1668, http://science.sciencemag.org/content/348/6237/895, 2015.

Alessandri, A., Catalano, F., Felice, M. D., Hurk, B. V. D., Reyes, F. D., Boussetta, S., Balsamo, G., and Miller, P. A.: Multi-scale enhancement of climate prediction over land by increasing the model sensitivity to vegetation variability in EC-Earth, Climate Dynamics, 49, 1215–1237, https://doi.org/10.1007/s00382-016-3372-4, https://link.springer.com/article/10.1007/s00382-016-3372-4, 2017.

Arino, O., Perez, J. J. R., Kalogirou, V., Bontemps, S., Defourny, P., and Bogaert, E. V.: Global Land Cover Map for 2009 (GlobCover 2009), PANGAEA, https://doi.org/10.1594/PANGAEA.787668, https://doi.org/10.1594/PANGAEA.787668, 2012.

Arneth, A., Miller, P. A., Scholze, M., Hickler, T., Schurgers, G., Smith, B., and Prentice, I. C.: CO2 inhibition of global terrestrial isoprene emissions: Potential implications for atmospheric chemistry, Geophysical Research Letters, 34, L18 813, https://doi.org/10.1029/2007GL030615, http://onlinelibrary.wiley.com/doi/10.1029/2007GL030615/abstract, 2007a.

Arneth, A., Niinemets, U., Pressley, S., Bäck, J., Hari, P., Karl, T., Noe, S., Prentice, I. C., Serça, D., Hickler, T., Wolf, A., and Smith, B.: Process-based estimates of terrestrial ecosystem isoprene emissions: incorporating the effects of a direct CO2-isoprene interaction, Atmos. Chem. Phys., 7, 31–53, https://doi.org/10.5194/acp-7-31-2007, https://www.atmos-chem-phys.net/7/31/2007/, 2007b.

Avitabile, V., Herold, M., Heuvelink, G. B. M., Lewis, S. L., Phillips, O. L., Asner, G. P., Armston, J., Ashton, P. S., Banin, L., Bayol, N., Berry, N. J., Boeckx, P., de Jong, B. H. J., DeVries, B., Girardin, C. A. J., Kearsley, E., Lindsell, J. A., Lopez-Gonzalez, G., Lucas, R., Malhi, Y., Morel, A., Mitchard, E. T. A., Nagy, L., Qie, L., Quinones, M. J., Ryan, C. M., Ferry, S. J. W., Sunderland, T., Laurin, G. V., Gatti, R. C., Valentini, R., Verbeeck, H., Wijaya, A., and Willcock, S.: An integrated pan-tropical biomass map using multiple reference datasets, Global Change Biology, 22, 1406–1420, https://doi.org/10.1111/gcb.13139, http://onlinelibrary.wiley.com/doi/10.1111/gcb.13139/abstract, 2016.

Baldauf, M., Seifert, A., Förstner, J., Majewski, D., Raschendorfer, M., and Reinhardt, T.: Operational Convective-Scale Numerical Weather Prediction with the COSMO Model: Description and Sensitivities, Monthly Weather Review, 139, 3887–3905, https://doi.org/10.1175/MWR-D-10-05013.1, https://journals.ametsoc.org/doi/10.1175/MWR-D-10-05013.1, 2011.

Baumgaertner, A. J. G., Jöckel, P., Kerkweg, A., Sander, R., and Tost, H.: Implementation of the Community Earth System Model (CESM) version 1.2.1 as a new base model into version 2.50 of the MESSy framework, Geosci. Model Dev., 9, 125–135, https://doi.org/10.5194/gmd-9-125-2016, https://www.geosci-model-dev.net/9/125/2016/, 2016.

CDO: Climate Data Operators, http://www.mpimet.mpg.de/cdo, 2018.

Ciais, P., Sabine, C., Bala, G., Bopp, L., Brovkin, V., Canadell, J., Chhabra, A., DeFries, R., Galloway, J., Heimann, M., Jones, C., Le Quéré, C., Myneni, R. B., Piao, S., and Thornton, P.: Carbon and Other Biogeochemical Cycles, in: Climate Change 2013: The Physical Science Basis. Contribution of Working Group I to the Fifth Assessment Report of the Intergovernmental Panel on Climate Change, pp. 465–570, Cambridge University Press, Cambridge, United Kingdom and New York, NY, USA., 2013.

Cox, P. M., Betts, R. A., Jones, C. D., Spall, S. A., and Totterdell, I. J.: Acceleration of global warming due to carbon-cycle feedbacks in a coupled climate model, Nature, 408, 184–187, https://doi.org/10.1038/35041539, https://www.nature.com/articles/35041539, 2000.

Dietmüller, S., Jöckel, P., Tost, H., Kunze, M., Gellhorn, C., Brinkop, S., Frömming, C., Ponater, M., Steil, B., Lauer, A., and Hendricks, J.: A new radiation infrastructure for the Modular Earth Submodel System (MESSy, based on version 2.51), Geosci. Model Dev., 9, 2209–2222, https://doi.org/10.5194/gmd-9-2209-2016, https://www.geosci-model-dev.net/9/2209/2016/, 2016.

Dimiceli, C., Carroll, M., Sohlberg, R., Kim, D. H., Kelly, M., and Townshend, J. G. R.: MOD44B MODIS/Terra Vegetation Continuous Fields Yearly L3 Global 250m SIN Grid V006. 2015, distributed by NASA EOSDIS Land Processes DAAC, https://doi.org//10.5067/MODIS/MOD44B.006, https://doi.org/10.5067/MODIS/MOD44B.006, 2015.

Flato, G., Marotzke, J., Abiodun, B., Braconnot, P., Chou, S. C., Collins, W. J., Cox, P., Driouech, F., Emori, S., Eyring, V., and Others: Evaluation of Climate Models., in: Climate Change 2013: The Physical Science Basis. Contribution of Working Group I to the Fifth Assessment Report of the Intergovernmental Panel on Climate Change, pp. 741–866, Cambridge University Press, Cambridge, United Kingdom and New York, NY, USA., 2013.

Forrest, M., Eronen, J. T., Utescher, T., Knorr, G., Stepanek, C., Lohmann, G., and Hickler, T.: Climate-vegetation modelling and fossil plant data suggest low atmospheric CO2 in the late Miocene, Clim. Past, 11, 1701–1732, https://doi.org/10.5194/cp-11-1701-2015, http://www.clim-past.net/11/1701/2015/, 2015.

Gerten, D., Schaphoff, S., Haberlandt, U., Lucht, W., and Sitch, S.: Terrestrial vegetation and water balance—hydrological evaluation of a dynamic global vegetation model, Journal of Hydrology, 286, 249–270, https://doi.org/10.1016/j.jhydrol.2003.09.029, http://www.sciencedirect.com/science/article/pii/S0022169403003901, 2004.

Haxeltine, A. and Prentice, I. C.: BIOME3: An equilibrium terrestrial biosphere model based on ecophysiological constraints, resource availability, and competition among plant functional types, Global Biogeochemical Cycles, 10, 693–709, https://doi.org/10.1029/96GB02344, http://onlinelibrary.wiley.com/doi/10.1029/96GB02344/abstract, 1996.

Hickler, T., Smith, B., Sykes, M. T., Davis, M. B., Sugita, S., and Walker, K.: Using a Generalized Vegetation Model to Simulate Vegetation Dynamics in Northeastern Usa, Ecology, 85, 519–530, https://doi.org/10.1890/02-0344, http://onlinelibrary.wiley.com/doi/10.1890/02-0344/abstract, 2004.

Hickler, T., Eklundh, L., Seaquist, J. W., Smith, B., Ardö, J., Olsson, L., Sykes, M. T., and Sjöström, M.: Precipitation controls Sahel greening trend, Geophysical Research Letters, 32, https://doi.org/10.1029/2005GL024370, https://agupubs.onlinelibrary.wiley.com/doi/abs/10.1029/2005GL024370, 2005.

Hickler, T., Prentice, I. C., Smith, B., Sykes, M. T., and Zaehle, S.: Implementing plant hydraulic architecture within the LPJ Dynamic Global Vegetation Model, Global Ecology and Biogeography, 15, 567–577, https://doi.org/10.1111/j.1466-8238.2006.00254.x, http://onlinelibrary.wiley.com/doi/10.1111/j.1466-8238.2006.00254.x/abstract, 2006.

Hickler, T., Smith, B., Prentice, I. C., MjöFors, K., Miller, P., Arneth, A., and Sykes, M. T.: CO_2 fertilization in temperate FACE experiments not representative of boreal and tropical forests, Global Change Biology, 14, 1531–1542, https://doi.org/10.1111/j.1365-2486.2008.01598.x, http://doi.wiley.com/10.1111/j.1365-2486.2008.01598.x, 2008.

Hickler, T., Vohland, K., Feehan, J., Miller, P. A., Smith, B., Costa, L., Giesecke, T., Fronzek, S., Carter, T. R., Cramer, W., Kühn, I., and Sykes, M. T.: Projecting the future distribution of European potential natural vegetation zones with a generalized, tree species-based dynamic vegetation model, Global Ecology and Biogeography, 21, 50–63, https://doi.org/10.1111/j.1466-8238.2010.00613.x, http://onlinelibrary.wiley.com/doi/10.1111/j.1466-8238.2010.00613.x/abstract, 2012.

Jones, P. W.: First- and Second-Order Conservative Remapping Schemes for Grids in Spherical Coordinates, Monthly Weather Review, 127, 2204–2210, https://doi.org/10.1175/1520-0493(1999)127<2204:FASOCR>2.0.CO;2, 1999.

Jöckel, P., Sander, R., Kerkweg, A., Tost, H., and Lelieveld, J.: Technical Note: The Modular Earth Submodel System (MESSy) - a new approach towards Earth System Modeling, Atmos. Chem. Phys., 5, 433–444, https://doi.org/10.5194/acp-5-433-2005, https://www.atmos-chem-phys.net/5/433/2005/, 2005.

Jöckel, P., Kerkweg, A., Pozzer, A., Sander, R., Tost, H., Riede, H., Baumgaertner, A., Gromov, S., and Kern, B.: Development cycle 2 of the Modular Earth Submodel System (MESSy2), Geosci. Model Dev., 3, 717–752, https://doi.org/10.5194/gmd-3-717-2010, https://www.geosci-model-dev.net/3/717/2010/, 2010.

Jöckel, P., Tost, H., Pozzer, A., Kunze, M., Kirner, O., Brenninkmeijer, C. A. M., Brinkop, S., Cai, D. S., Dyroff, C., Eckstein, J., Frank, F., Garny, H., Gottschaldt, K.-D., Graf, P., Grewe, V., Kerkweg, A., Kern, B., Matthes, S., Mertens, M., Meul, S., Neumaier, M., Nützel, M., Oberländer-Hayn, S., Ruhnke, R., Runde, T., Sander, R., Scharffe, D., and Zahn, A.: Earth System Chemistry integrated Modelling (ESCiMo) with the Modular Earth Submodel System (MESSy) version 2.51, Geosci. Model Dev., 9, 1153–1200, https://doi.org/10.5194/gmd-9-1153-2016, https://www.geosci-model-dev.net/9/1153/2016/, 2016.

Kelley, D. I., Prentice, I. C., Harrison, S. P., Wang, H., Simard, M., Fisher, J. B., and Willis, K. O.: A comprehensive benchmarking system for evaluating global vegetation models, Biogeosciences, 10, 3313–3340, https://doi.org/10.5194/bg-10-3313-2013, http://www.biogeosciences.net/10/3313/2013/, 2013.

Kerkweg, A., Hofmann, C., Jöckel, P., Mertens, M., and Pante, G.: The on-line coupled atmospheric chemistry model system MECO(n) – Part 5: Expanding the Multi-Model-Driver (MMD v2.0) for 2-way data exchange including data interpolation via GRID (v1.0), Geosci. Model Dev., 11, 1059–1076, https://doi.org/10.5194/gmd-11-1059-2018, https://www.geosci-model-dev.net/11/1059/2018/, 2018.

Kern, B.: Chemical interaction between ocean and atmosphere, http://ubm.opus.hbz-nrw.de/volltexte/2014/3732, 2013.

Knorr, W., Jiang, L., and Arneth, A.: Climate, CO2 and human population impacts on global wildfire emissions, Biogeosciences, 13, 267–282, https://doi.org/10.5194/bg-13-267-2016, https://www.biogeosciences.net/13/267/2016/, 2016.

Lamarque, J.-F., Dentener, F., McConnell, J., Ro, C.-U., Shaw, M., Vet, R., Bergmann, D., Cameron-Smith, P., Dalsoren, S., Doherty, R., Faluvegi, G., Ghan, S. J., Josse, B., Lee, Y. H., MacKenzie, I. A., Plummer, D., Shindell, D. T., Skeie, R. B., Stevenson, D. S., Strode, S., Zeng, G., Curran, M., Dahl-Jensen, D., Das, S., Fritzsche, D., and Nolan, M.: Multi-model mean nitrogen and sulfur deposition from the Atmospheric Chemistry and Climate Model Intercomparison Project (ACCMIP): evaluation of historical and projected future changes, Atmos. Chem. Phys., 13, 7997–8018, https://doi.org/10.5194/acp-13-7997-2013, https://www.atmos-chem-phys.net/13/7997/2013/, 2013.

Lehsten, V., Tansey, K., Balzter, H., Thonicke, K., Spessa, A., Weber, U., Smith, B., and Arneth, A.: Estimating carbon emissions from African wildfires, Biogeosciences, 6, 349–360, https://doi.org/10.5194/bg-6-349-2009, https://www.biogeosciences.net/6/349/2009/, 2009.

Lindeskog, M., Arneth, A., Bondeau, A., Waha, K., Seaquist, J., Olin, S., and Smith, B.: Implications of accounting for land use in simulations of ecosystem carbon cycling in Africa, Earth Syst. Dynam., 4, 385–407, https://doi.org/10.5194/esd-4-385-2013, http://www.earth-syst-dynam.net/4/385/2013/, 2013.

Lucht, W., Prentice, I. C., Myneni, R. B., Sitch, S., Friedlingstein, P., Cramer, W., Bousquet, P., Buermann, W., and Smith, B.: Climatic Control of the High-Latitude Vegetation Greening Trend and Pinatubo Effect, Science, 296, 1687–1689, https://doi.org/10.1126/science.1071828, http://science.sciencemag.org/content/296/5573/1687, 2002.

Medlyn, B. E., Zaehle, S., De Kauwe, M. G., Walker, A. P., Dietze, M. C., Hanson, P. J., Hickler, T., Jain, A. K., Luo, Y., Parton, W., Prentice, I. C., Thornton, P. E., Wang, S., Wang, Y.-P., Weng, E., Iversen, C. M., McCarthy, H. R., Warren, J. M., Oren, R., and Norby, R. J.:

Using ecosystem experiments to improve vegetation models, Nature Climate Change, 5, 528–534, https://doi.org/10.1038/nclimate2621, https://www.nature.com/articles/nclimate2621, 2015.

Miller, P. A. and Smith, B.: Modelling Tundra Vegetation Response to Recent Arctic Warming, AMBIO, 41, 281–291, https://doi.org/10.1007/s13280-012-0306-1, https://link.springer.com/article/10.1007/s13280-012-0306-1, 2012.

Pozzer, A., Jöckel, P., Kern, B., and Haak, H.: The Atmosphere-Ocean General Circulation Model EMAC-MPIOM, Geosci. Model Dev., 4, 771–784, https://doi.org/10.5194/gmd-4-771-2011, https://www.geosci-model-dev.net/4/771/2011/, 2011.

Rabin, S. S., Melton, J. R., Lasslop, G., Bachelet, D., Forrest, M., Hantson, S., Kaplan, J. O., Li, F., Mangeon, S., Ward, D. S., Yue, C., Arora, V. K., Hickler, T., Kloster, S., Knorr, W., Nieradzik, L., Spessa, A., Folberth, G. A., Sheehan, T., Voulgarakis, A., Kelley, D. I., Prentice, I. C., Sitch, S., Harrison, S., and Arneth, A.: The Fire Modeling Intercomparison Project (FireMIP), phase 1: experimental and analytical protocols with detailed model descriptions, Geosci. Model Dev., 10, 1175–1197, https://doi.org/10.5194/gmd-10-1175-2017, http://www.geosci-model-dev.net/10/1175/2017/, 2017.

Roeckner, E., Brokopf, R., Esch, M., Giorgetta, M., Hagemann, S., Kornblueh, L., Manzini, E., Schlese, U., and Schulzweida, U.: Sensitivity of Simulated Climate to Horizontal and Vertical Resolution in the ECHAM5 Atmosphere Model, Journal of Climate, 19, 3771–3791, https://doi.org/10.1175/JCLI3824.1, http://journals.ametsoc.org/doi/full/10.1175/JCLI3824.1, 2006.

Simard, M., Pinto, N., Fisher, J. B., and Baccini, A.: Mapping forest canopy height globally with spaceborne lidar, Journal of Geophysical Research: Biogeosciences, 116, G04 021, https://doi.org/10.1029/2011JG001708, http://onlinelibrary.wiley.com/doi/10.1029/2011JG001708/abstract, 2011.

Sitch, S., Smith, B., Prentice, I. C., Arneth, A., Bondeau, A., Cramer, W., Kaplan, J. O., Levis, S., Lucht, W., Sykes, M. T., Thonicke, K., and Venevsky, S.: Evaluation of ecosystem dynamics, plant geography and terrestrial carbon cycling in the LPJ dynamic global vegetation model, Global Change Biology, 9, 161–185, https://doi.org/10.1046/j.1365-2486.2003.00569.x, http://onlinelibrary.wiley.com/doi/10.1046/j.1365-2486.2003.00569.x/abstract, 2003.

Smith, B., Prentice, I. C., and Sykes, M. T.: Representation of vegetation dynamics in the modelling of terrestrial ecosystems: comparing two contrasting approaches within European climate space, Global Ecology and Biogeography, 10, 621–637, https://doi.org/10.1046/j.1466-822X.2001.t01-1-00256.x, http://onlinelibrary.wiley.com/doi/10.1046/j.1466-822X.2001.t01-1-00256.x/abstract, 2001.

Smith, B., Samuelsson, P., Wramneby, A., and Rummukainen, M.: A model of the coupled dynamics of climate, vegetation and terrestrial ecosystem biogeochemistry for regional applications, Tellus A, 63, 87–106, https://doi.org/10.1111/j.1600-0870.2010.00477.x, https://onlinelibrary.wiley.com/doi/abs/10.1111/j.1600-0870.2010.00477.x, 2011.

Smith, B., Wårlind, D., Arneth, A., Hickler, T., Leadley, P., Siltberg, J., and Zaehle, S.: Implications of incorporating N cycling and N limitations on primary production in an individual-based dynamic vegetation model, Biogeosciences, 11, 2027–2054, https://doi.org/10.5194/bg-11-2027-2014, http://www.biogeosciences.net/11/2027/2014/, 2014.

Taylor, K. E., Williamson, D., and Zwiers, F.: The sea surface temperature and sea-ice concentration boundary conditions for AMIP II simulations, Program for Climate Model Diagnosis and Intercomparison, Lawrence Livermore National Laboratory, University of California, 2000.

Thonicke, K., Venevsky, S., Sitch, S., and Cramer, W.: The role of fire disturbance for global vegetation dynamics: coupling fire into a Dynamic Global Vegetation Model, Global Ecology and Biogeography, 10, 661–677, https://doi.org/10.1046/j.1466-822X.2001.00175.x, http://onlinelibrary.wiley.com/doi/10.1046/j.1466-822X.2001.00175.x/abstract, 2001.

Thonicke, K., Spessa, A., Prentice, I. C., Harrison, S. P., Dong, L., and Carmona-Moreno, C.: The influence of vegetation, fire spread and fire behaviour on biomass burning and trace gas emissions: results from a process-based model, Biogeosciences, 7, 1991–2011, https://doi.org/10.5194/bg-7-1991-2010, http://www.biogeosciences.net/7/1991/2010/, 2010.

Thurner, M., Beer, C., Santoro, M., Carvalhais, N., Wutzler, T., Schepaschenko, D., Shvidenko, A., Kompter, E., Ahrens, B., Levick, S. R., and Schmullius, C.: Carbon stock and density of northern boreal and temperate forests, Global Ecology and Biogeography, 23, 297–310, https://doi.org/10.1111/geb.12125, http://onlinelibrary.wiley.com/doi/10.1111/geb.12125/abstract, 2014.

Tost, H.: Chemistry–climate interactions of aerosol nitrate from lightning, Atmos. Chem. Phys., 17, 1125–1142, https://doi.org/10.5194/acp-17-1125-2017, https://www.atmos-chem-phys.net/17/1125/2017/, 2017.

Tost, H., Jöckel, P., and Lelieveld, J.: Influence of different convection parameterisations in a GCM, Atmos. Chem. Phys., 6, 5475–5493, https://doi.org/10.5194/acp-6-5475-2006, https://www.atmos-chem-phys.net/6/5475/2006/, 2006.

Tost, H., Forrest, M., and Hickler, T.: Interactive vegetation influences on climatological meteorological fields and trace gas emissions, vol. 20, p. 12047, http://adsabs.harvard.edu/abs/2018EGUGA..2012047T, 2018.

Wei, Y., Liu, S., Huntzinger, D. N., Michalak, A. M., Viovy, N., Post, W. M., Schwalm, C. R., Schaefer, K., Jacobson, A. R., Lu, C., Tian, H., Ricciuto, D. M., Cook, R. B., Mao, J., and Shi, X.: The North American Carbon Program Multi-scale Synthesis and Terrestrial Model Intercomparison Project – Part 2: Environmental driver data, Geoscientific Model Development, 7, 2875–2893, https://doi.org/https://doi.org/10.5194/gmd-7-2875-2014, https://www.geosci-model-dev.net/7/2875/2014/, 2014.

Weiss, M., Miller, P. A., van den Hurk, B. J. J. M., van Noije, T., Ştefănescu, S., Haarsma, R., van Ulft, L. H., Hazeleger, W., Le Sager, P., Smith, B., and Schurgers, G.: Contribution of Dynamic Vegetation Phenology to Decadal Climate Predictability, Journal of Climate, 27, 8563–8577, https://doi.org/10.1175/JCLI-D-13-00684.1, https://journals.ametsoc.org/doi/abs/10.1175/JCLI-D-13-00684.1, 2014.

Wramneby, A., Smith, B., and Samuelsson, P.: Hot spots of vegetation-climate feedbacks under future greenhouse forcing in Europe, Journal of Geophysical Research, 115, https://doi.org/10.1029/2010JD014307, http://doi.wiley.com/10.1029/2010JD014307, 2010.

Zaehle, S., Sitch, S., Smith, B., and Hatterman, F.: Effects of parameter uncertainties on the modeling of terrestrial biosphere dynamics, Global Biogeochemical Cycles, 19, GB3020, https://doi.org/10.1029/2004GB002395, http://onlinelibrary.wiley.com/doi/10.1029/2004GB002395/abstract, 2005.

Zaehle, S., Medlyn, B. E., De Kauwe, M. G., Walker, A. P., Dietze, M. C., Hickler, T., Luo, Y., Wang, Y.-P., El-Masri, B., Thornton, P., Jain, A., Wang, S., Warlind, D., Weng, E., Parton, W., Iversen, C. M., Gallet-Budynek, A., McCarthy, H., Finzi, A., Hanson, P. J., Prentice, I. C., Oren, R., and Norby, R. J.: Evaluation of 11 terrestrial carbon–nitrogen cycle models against observations from two temperate Free-Air CO2 Enrichment studies, New Phytologist, 202, 803–822, https://doi.org/10.1111/nph.12697, https://nph.onlinelibrary.wiley.com/doi/full/10.1111/nph.12697, 2014.

Zhang, W., Jansson, C., Miller, P. A., Smith, B., and Samuelsson, P.: Biogeophysical feedbacks enhance the Arctic terrestrial carbon sink in regional Earth system dynamics, Biogeosciences, 11, 5503–5519, https://doi.org/10.5194/bg-11-5503-2014, https://www.biogeosciences.net/11/5503/2014/, 2014.